

See discussions, stats, and author profiles for this publication at: <https://www.researchgate.net/publication/280998962>

Tuning Properties in Silver Clusters

ARTICLE *in* JOURNAL OF PHYSICAL CHEMISTRY LETTERS · AUGUST 2015

Impact Factor: 7.46 · DOI: 10.1021/acs.jpclett.5b00934 · Source: PubMed

CITATIONS

2

READS

38

3 AUTHORS, INCLUDING:



Megalamane Siddaramappa Bootharaju

King Abdullah University of Science and Techn...

24 PUBLICATIONS 464 CITATIONS

[SEE PROFILE](#)



Osman M Bakr

King Abdullah University of Science and Techn...

72 PUBLICATIONS 1,103 CITATIONS

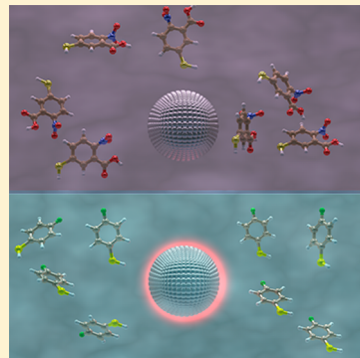
[SEE PROFILE](#)

Tuning Properties in Silver Clusters

Chakra P. Joshi, Megalamane S. Bootharaju, and Osman M. Bakr*

Division of Physical Sciences and Engineering, Solar and Photovoltaics Engineering Research Center, King Abdullah University of Science and Technology (KAUST), Thuwal 23955-6900, Saudi Arabia

ABSTRACT: The properties of Ag nanoclusters are not as well understood as those of their more precious Au cousins. However, a recent surge in the exploration of strategies to tune the physicochemical characteristics of Ag clusters addresses this imbalance, leading to new insights into their optical, luminescence, crystal habit, metal-core, ligand-shell, and environmental properties. In this Perspective, we provide an overview of the latest strategies along with a brief introduction of the theoretical framework necessary to understand the properties of silver nanoclusters and the basis for their tuning. The advances in cluster research and the future prospects presented in this Perspective will eventually guide the next large systematic study of nanoclusters, resulting in a single collection of data similar to the periodic table of elements.



The discovery of the periodic table and the subsequent understanding of atomic properties of elements in the early 20th century initiated many exciting research areas in chemistry. These areas laid the foundation of the cluster field which came into being decades later, that is, the exploration of the properties of new exotic species consisting of a few to hundreds of atoms known as giant atoms, superatoms, magic clusters, or simply clusters.^{1–7} The uncommon characteristics associated with these clusters were highlighted by Richard Feynman in his famous lecture at the American Physical Society meeting in 1959.¹ Around the same time, Becker et al.² experimentally demonstrated the possibility for control over atomic/molecular clusters. These clusters are fascinating not only because of their small size but also because of their resemblance to molecules. Later developments of sophisticated instruments and experimental designs in the 1980s helped characterize metal and nonmetal clusters, such as Na_n⁸ and fullerene C₆₀⁹, with unprecedented atomic precision. Despite having the same carbon building block as coal, graphite, and diamond, fullerene C₆₀ exhibits unusual properties, which motivated the cluster community to find analogies in other systems. In the meantime, advances in theoretical and computational modeling of these clusters aided in breathtaking developments in cluster science.

Although metal clusters are considered a part of the broader class of metal nanoparticles (NPs), they have a much shorter history and their manifested characteristics may only be understood based on quantized electronic interactions. However, metal NPs of tens to hundreds of nanometers have been used by artists since the Middle Ages and before to stain glass with colorful hues. Although these artisans were unaware of the exact source and nanoscale nature of the material that helped emanate these beautiful colors, later plasmonic NPs were observed to cause these phenomena.^{10,11}

In 1857, Faraday reported the first formal synthesis of metal NPs, that is, the synthesis of a red Au NP solution.¹² He immediately attributed the color of the solution to the size of the Au particles even though he lacked evidence to substantiate this hypothesis. Almost a century later in 1951, with the arrival of electron microscopy, Turkevich et al.¹³ proved Faraday's prediction correct and observed ~3–10 nm NPs. Around the same time, McPartlin et al.¹⁴ reported ultrasmall Au NPs, that is, [Au₁₁(PPh₃)₃(SCN)₃] with sizes of ~1 nm. Notably, both Faraday's Au NPs¹² and the Au₁₁ cluster^{14,15} produced a similar red solution despite their drastically different sizes. The red appearance of Faraday's NPs^{11,13} was attributed to surface plasmons, whereas molecular-like electronic transitions¹⁵ were thought to cause the reddening of the Au₁₁ cluster solution.

Following the footsteps of Brust et al.,¹⁶ Whetten and co-workers^{5,6,17} reported the synthesis of 5.6, 8.7, 10.4, and 29 kDa Au species/clusters in their work of late 1990s and early 2000s, coining the concept of gold NP "molecules". However, purification and complete isolation of these ~1–2 nm clusters remained elusive, resulting in a poor estimation of their precise molecular formula.⁵ Successive work by the Tsukuda group³ in a similar system led to the isolation and unambiguous determination of the molecular formula of several magic gold-glutathione Au_n(SG)_n species, including Au₁₀(SG)₁₀, Au₁₅(SG)₁₃, Au₁₈(SG)₁₄, Au₂₂(SG)₁₆, Au₂₂(SG)₁₇, Au₂₅(SG)₁₈, Au₂₉(SG)₂₀, Au₃₃(SG)₂₂, and Au₃₉(SG)₂₄. This seminal work in the mid 2000s by the Tsukuda group³ spurred research on Au clusters and on other metal compositions.

After Au, Ag was an obvious candidate because of its low price, largely unexplored properties, and shared similarities with Au, despite its notorious lack of stability. A few unconfirmed

Received: May 5, 2015

Accepted: July 9, 2015

Published: July 9, 2015

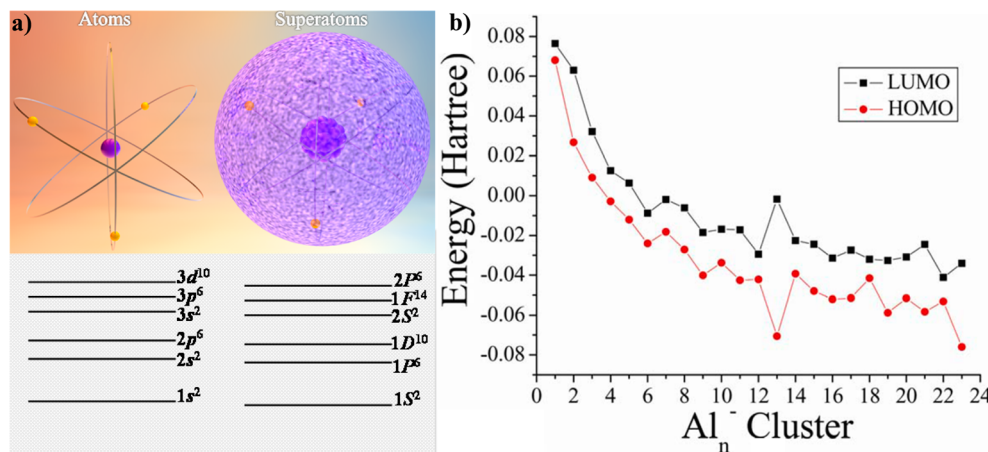
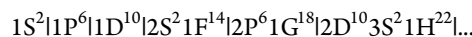


Figure 1. (a) Cartoon showing the electron orbitals of an atom (lowercase s, p, d, ...) and superatom (uppercase S, P, D, ...) with a confined and smeared nuclear region and (b) Theoretical plot of energy associated with the HOMO and LUMO levels of Al_n^- clusters as a function of size.³² Panel b is reprinted from ref 32 with permission.

reports focused on the precise composition of Ag NPs;^{18,19} however, in the late 2000s, Bakr and Stellacci et al.²⁰ discovered Ag NPs with precise formula that displayed nonplasmonic nature.²¹ These nonplasmonic Ag NPs were called IBANs (Intensely and Broadly Absorbing Ag NPs).²⁰ Analogous to the $\text{Au}_m(\text{SG})_n$ species, IBANs have a precise molecular formula of $[\text{Ag}_{44}(\text{SR})_{30}]^{-4}$ and are <2 nm in size.^{20,21} Since then, a handful of precise thiolated Ag clusters have been characterized with atomic precision.^{4,22–26} For example, recent work on the glutathione Ag system by the Bigioni group led to the isolation of various magic $\text{Ag}_m(\text{SG})_n$ species that mostly remained uncharacterized except for the $\text{Ag}_{32}(\text{SG})_{19}$ species.²³ A species with similar optical spectrum as $\text{Ag}_{32}(\text{SG})_{19}$ was assigned by Bertorelle et al.²² as $\text{Ag}_{31}(\text{SG})_{19}$. This discrepancy in the mass characterization of similar optical species may be due to the ease of fragmentation and rearrangement of atoms in the gas phase in a mass spectrometer. However, the structure could be decisively determined in the solid state using single-crystal X-ray diffraction if the cluster could be successfully crystallized. Thus, the ground-breaking work of the Kornberg group,²⁷ which revealed the crystal structure of $\text{Au}_{102}(p\text{-MBA})_{44}$, paved the way for subsequent crystal structure determination of other metal clusters, such as $\text{Ag}_{44}(p\text{-MBA})_{30}$ ²⁸ and $\text{Ag}_{44}(\text{SPhF}_2)_{30}$ ²⁹ with a charge of -4 . This landmark achievement not only revealed the molecular structure and metal–thiolate interface of the clusters with unprecedented detail but also provided enormous impetus for the explosive growth in the theoretical and computational fields to understand and predict the fundamental properties associated with the existing and emerging metal clusters.

Decades earlier, before the actual crystallization of the thiol-protected Au/Ag clusters,^{27–29} significant theoretical work was performed to understand and predict the properties of bare metal clusters and was known as the superatom theory.^{8,30,31} These gas-phase metal clusters were assumed to behave like giant atoms and therefore follow the same rules as atoms, such as orbital hybridization, Hund's rule, and the Aufbau principle. Therefore, superatom theory is no different from atomic theory even though superatoms are composed of a few tens to thousands of atoms and have the Jellium foundation.^{8,30} The Jellium model assumes that positive charges are spread evenly over the sphere and are inert (Figure 1a).^{8,30} This assumption indeed qualitatively explained various properties related to superatoms.^{8,31}

For instance, consider the Na_n cluster. Sodium has one 3s electron in its valence shell and is known to form bare Na_n clusters in the gas phase.⁸ Following the observation that some Na_n species were more stable than others, Knight and co-workers⁸ rationalized this discrepancy based on the electronic shell-closing rule of the superatom theory, where large HOMO–LUMO gaps created by a closed shell conferred stability to bare Na_n clusters analogous to those of inert gases. The resemblance between the filling of the superatomic orbitals of these bare metal clusters to the filling of atoms inspired Häkkinen's group³³ to extend this idea to ligand-protected metal clusters that follow the electronic shell closure rule described below:^{31,33}



where the vertical lines indicate a shell-closure with a very large HOMO–LUMO gap. The uppercase characters S, P, D, F, ... represent the angular momentum quantum numbers of the superatomic orbitals, and 1, 2, 3, ... correspond to radial nodes. Using the electronic shell-closing rule, one can obtain closed shells for $n_e = 2, 8, 18, 20, 34, 40, 58, \dots$, where n_e is the total free electrons available in a cluster.³³ For example, the stability of Na_{40} and Al_{13}^- clusters^{8,34} can be explained based on the electronic shell closure. The Na_{40} and Al_{13}^- clusters^{8,34} contain 40 Na(3s¹) and 13 Al(3s²3p¹) atoms, resulting in a total of 40 and 39 valence electrons, respectively. The inclusion of a negative charge associated with the Al_{13}^- cluster results in a total of 40 valence electrons. This electron count corresponds to a closed shell ($n_e = 40$) with a configuration of 1S², 1P⁶, 1D¹⁰, 2S², 1F¹⁴, 2P⁶ imparting exceptional stability to these gas phase clusters (Figure 1b).

Although the electronic shell-closing rule is useful in explaining the stability of clusters, it also suggests the existence of a limited number of stable clusters with closed electronic shells. Research work by Brust and co-workers on Au–thiolates provided some insights to stabilize clusters' metal core with ligands.¹⁶ However, this idea was later viewed more generally as describing a metal core that can coordinate, deposit, or access electrons from an electron reservoir in the form of surface ligands to maintain a coveted closed electronic shell, thereby ensuring stability. The idea of ligands as a surrounding electron reservoir then spread to Ag and other metals,^{4,5,19} where ligands are believed to satisfy the dangling bonds present on a cluster.¹⁶

By considering ligand and metal–core interactions, Walter et al.³³ proposed an electron count magic rule for ligand-protected metal clusters. According to the rule, for the ligand-protected Ag clusters of the form $[C_xAg_NL_M]^z$, where C is a Lewis-base-type coordinating ligand that does not withdraw electrons but rather bonds to a metal core through a dative bond (e.g., phosphine and amine), and L is a one-electron-withdrawing ligand (e.g., thiol), the electron-count rule is³³

$$n_e = Nv - M - z$$

where v is the atomic valence of Ag, N is the number of core Ag atoms, M and x are the number of respective ligands, and z is the overall charge of the cluster. The application of the electron-count rule to condensed-phase metal clusters explains why $[Au_{25}(SG)_{18}]^{-4}$ ³⁵ and $[Ag_{44}(SR)_{30}]^{-4}$ ^{28,29}, with $n_e = 8$ and 18-electron cores, respectively, are very stable as their total free electron counts correspond to closed electronic shells.³³

Despite the success of the electronic shell closure, the presence of conspicuous mass peaks of bare metal clusters, such as Na_{12} , Na_{26} , and Na_{38} , in the gas phase⁸ and stable ligand-protected metal clusters, such as $Au_{38}(SR)_{24}$,³⁶ $Ag_{32}(SG)_{19}$,^{23,37} and $Ag_{15}(SG)_{11}$,²² in the condensed phase appear to be exceptions to the rule. However, Clemenger attributed the stability of these Na_n clusters to their nonspherical shape caused by a distortion analogous to the Jahn–Teller effect^{31,38} that could be extended to condensed phase clusters. Indeed, $Au_{38}(SR)_{24}$ with a 14-electron core was later crystallized³⁶ and observed to have a nonspherical shape (prolate, face-fused bi-icosahedron). Similar nonspherical shapes are expected for $Ag_{32}(SG)_{19}$,²³ $Ag_{31}(SG)_{19}$, and $Ag_{15}(SG)_{11}$.²²

In addition to electronic shell closing, geometric shell closing is also applied to explain the cluster stability. Depending on the geometric shape, for example, cubic, tetrahedral, octahedral, or icosahedral, certain numbers of building units are required to form a closed geometry. Consider a cubic shape. It is not possible to construct a cube out of 26 or 28 spheres; this goal requires precisely 27 atoms (i.e., 3^3). This type of precise requirement can be observed in the fullerene C_{60} with icosahedral symmetry.⁹ Fullerene is known to have a closed geometry and hence is very stable.⁹ Removing or adding an extra carbon atom to the C_{60} surface would destabilize the geometry and therefore requires significant energy. Likewise, metal clusters also prefer icosahedral symmetry at the core.^{7,28,29} The number of atoms required to make a closed icosahedral geometry can be determined using Mackay's³⁹ icosahedral sequence $S_n = 10n^2 + 2$, where S_n represents the surface atoms of the n^{th} shell, from which one can acquire a

closed geometric shell configuration corresponding to 1, 13, 55, 147, 309, 561, ... core atoms. Leuchtner et al.³⁴ experimentally demonstrated the importance of geometric shell by studying the reactivity of Al_{13}^- , Al_{23}^- , and Al_{37}^- clusters (representing 40, 70, and 112 electrons, respectively) toward oxygen. Although all three clusters have a closed electronic shell, Al_{13}^- was observed to be the most stable³⁴ because of its closed geometric shell (13-atom icosahedron, Figure 1b). Similar stability was reported for Ag_{13}^- clusters.⁴⁰ The open geometry associated with Al_{23}^- and Al_{37}^- ³⁴ would sustain steps on these cluster surfaces, lowering the work function and, hence, reducing the stability.⁴¹ For practical realization of these theories, actual clusters must be synthesized.

Geometric shell closing is also applied to explain the cluster stability. Depending on the geometric shape, for example, cubic, tetrahedral, octahedral, or icosahedral, certain numbers of building units are required to form a closed geometry.

Syntheses of Ag Clusters. The synthesis protocol for ligand-protected Ag clusters is rather straightforward. Generally, a Ag salt is mixed with a thiol ligand in a suitable solvent system to form a silver-thiolate complex. The silver-thiolate complex is then reduced with a strong reducing agent, such as $NaBH_4$, to produce Ag clusters that are successively washed and then redispersed in an appropriate solvent. Other synthetic routes, such as solid-state,⁴² ligand-exchange,⁴³ and antagalvanic processes,⁴⁴ are also available. Some aqueous syntheses produce polydispersed Ag clusters such as $Ag_m(SG)_n$ clusters,^{4,19} whose purity and monodispersity are achieved either via cyclic reduction under oxidative conditions or through polyacrylamide gel electrophoresis (PAGE). By contrast, the monodispersity of organic soluble clusters, especially alloys, is improved via thermal processing²⁹ or chromatography.^{45–47} Nevertheless, by tailoring the properties of the solvents and ligands, some remarkable success has been achieved in obtaining a truly single-sized product of Ag clusters in both aqueous and organic phases using one-pot synthesis approaches.^{20,28,29,48,49} This scaling up of cluster synthesis with no known upper limit (irrespective of pure or doped clusters, Figure 2) reminds us of



Figure 2. Scaled-up final single-sized product of (a) $[Ag_{44}(p\text{-MBA})_{30}]^{-4}$, 140 g;²⁸ (b) $[Ag_{44}(SPhF)_{30}]^{-4}$, 10.89 g;²⁹ (c) $[Ag_{44}(MNBA)_{30}]^{-4}$ clusters, 172 mg in 1 L of 1 M aqueous NaOH;⁴⁸ and (d) $Au_{25}Ag_2(PET)_{18}$ alloy cluster, 0.86 g.⁴⁹ Adapted from refs 28, 29, 48, and 49 with permission.

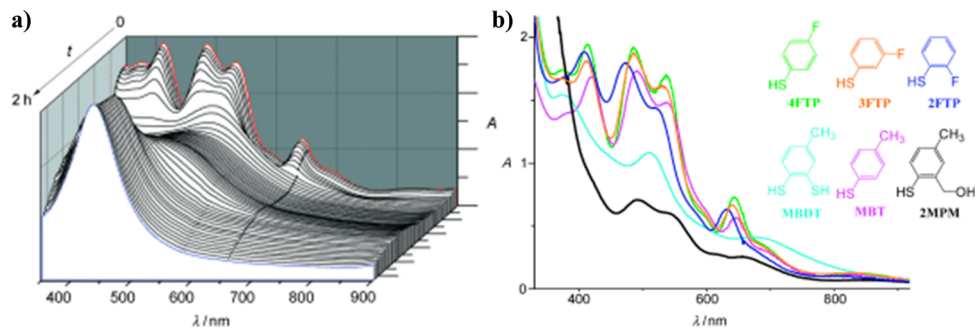


Figure 3. (a) Optical spectra of $[Ag_{44}(SR)_{30}]^{-4}$ clusters at 90 °C as a function of time²⁰ and (b) effect of various aryl-thiol ligands on the optical spectra of Ag clusters.²⁰ Reprinted from ref 20 with permission.

the molecular nature of these clusters and could facilitate the application of clusters in photocatalysis⁵⁰ and sensing^{24,25} over large areas in addition to improving the fundamental understanding of their properties.

Factors Involved in Tuning the Properties of Ag Clusters. The physical and chemical properties of clusters are affected by their cores, ligands, and environments. By varying these factors, it is possible to tune the cluster properties. To illustrate, consider the family of magic $Ag_m(SG)_n$ clusters.^{4,51} While synthesizing the family of glutathione Ag clusters, the same environment was sustained in a reaction vessel; however, clusters purified from the gel exhibited distinct optical properties. This behavior is possible because of the different core sizes, that is, the number of Ag atoms changed from one cluster to another. However, it is expected that the change in core atoms would subsequently lead to a different number of ligands to enclose the core appropriately, which was also observed with $Ag_m(SG)_n$ ³ and $Ag_m(PET)_n$ ⁷ clusters (PET: 2-phenylethanethiol), where a quantitative relationship was mapped between the cluster cores and their optical properties.

The properties arising from the cluster core can also be engineered by doping or alloying the cluster with other metal atoms, resulting in combined properties from both metal atoms. In general, doped clusters are synthesized by reducing a suitable ratio of different metal salt precursors in the presence of a ligand. The Zheng group²⁹ reported the doping of $[Ag_{44}(SPhF_2)_{30}]^{-4}$ with 12-Au atoms, producing completely different properties. For example, the optical spectrum of $[Ag_{44}(SPhF_2)_{30}]^{-4}$ contained eight peaks, including two shoulder peaks, and the cluster was stable for <4 h,²⁹ whereas the spectrum of its 12-Au-doped counterpart, $[Ag_{32}Au_{12}(SPhF_2)_{30}]^{-4}$, contained only two prominent and three shoulder peaks, and the cluster was able to survive >12 h under the harsh conditions of 80 °C.²⁹ In contrast, the Dass group⁵² reported selective replacement of 12-Au atoms of a $[Au_{25}(PET)_{18}]^{-}$ core with Ag, producing a mixture of $[Au_{25-x}Ag_x(PET)_{18}]^{-}$ alloy clusters. These researchers also noticed a significant change in the optical properties of $[Au_{25}(PET)_{18}]^{-}$ clusters after doping. Fortunately, the core size was preserved in both cases after being alloyed with different metal atoms. Like Au, Ag mingles with other metals, such as Pd, Pt, and Ni, at the nanoscale, producing alloy clusters with various compositions, such as $[Ag_5Pd_4(SePh)_{12}]^{-}$,⁴⁵ $Ag_4Pt_2(DMSA)_4$,⁴⁷ and $Ag_4Ni_2(DMSA)_4$.⁴⁶ The syntheses of materials of this type with different metal precursors are challenging and often lead to a mixture of clusters with different metal ratios, which are extremely difficult to purify.

Galvanic exchange is also used for alloying clusters. In this process, usually a metal cluster is mixed with salt or a cluster of

another metal, causing a redox reaction to occur. Using this technique, the Pradeep group⁵³ succeeded in producing a luminescent alloy cluster $Ag_7Au_6(MSA)_{10}$ by reacting a mixture of $Ag_7(MSA)_7$ and $Ag_8(MSA)_8$ clusters with Au^{3+} ions of aqueous $HAuCl_4$. These researchers proposed that the Au^{3+} ions first formed $Au(I)$ -thiolates with excess MSA (mercapto-succinic acid) that subsequently reacted with the cluster mixture Ag_{7-8} , forming the luminescent cluster $Ag_7Au_6(MSA)_{10}$. In addition to galvanic exchange, the antagalvanic process was also observed to be equally effective for alloying the clusters. The Wu group⁴⁹ succeeded in alloying $[Au_{25}(PET)_{18}]^{-}$ clusters with Ag simply by mixing $[Au_{25}(PET)_{18}]^{-}$ clusters with Ag^+ in $AgNO_3$ solutions, producing luminescent $[Au_{25}Ag_2(PET)_{18}]^{-}$ clusters. In this case, the $[Au_{25}(PET)_{18}]^{-}$ clusters reduced the Ag^+ to Ag atoms, thereby resulting in successful alloying. Although both the galvanic and antagalvanic processes produced luminescence clusters, in both cases, the cluster size unfortunately changed because of the alloying, which complicates the determination of the most crucial factors affecting the cluster properties. Nonetheless, this reactivity of the clusters in the galvanic/antagalvanic process stems from the reduction potential of the metals, which decreases drastically with the core size.⁵⁴ For instance, the standard reduction potential of bulk Ag changed from +0.79 to -1.8 V when its size reached an isolated Ag atom in aqueous solution.⁵⁴ This dramatic change in the reduction potential makes clusters attractive for the galvanic and antagalvanic processes.

The environment where the clusters originate or are placed is also an important factor that contributes to their overall characteristics. Some environmental factors, such as temperature,⁵⁵ pH,^{22,51} and the solvent,⁵⁶ are known to change the cluster properties. For example, the Ras group⁵⁶ demonstrated a dramatic change in the luminescence of Ag clusters, supposedly Ag_2 and Ag_3 , by changing the solvent type or using cosolvents. Although the reported Ag_2 and Ag_3 are more likely the fragments (in the mass measurement during mass spectrometry) of a larger Ag cluster, the observed luminescence tunability highlighted the important role of environmental changes. In the same manner, the Mak group⁵⁵ demonstrated the luminescence tunability of Ag_{12} clusters. Likewise, the Stellacci group^{20,21} demonstrated the optical tunability of Ag_{44} clusters simply by raising the temperature (Figure 3a). The optical tunability of Ag_{44} clusters with temperature actually caused Ag-core growth, producing plasmonic NPs.²⁰ Despite the aforementioned environmental factors, such as solvato-chromism⁵⁶ and thermochromism,⁵⁵ a complete understanding of how the environment affects the cluster properties has not yet been achieved.

The ligand is another factor that changes the cluster properties. The compatibility of a cluster toward a particular solvent largely depends on the ligand. Moreover, the cluster stability depends on how well the ligands guard a sensitive core from the surrounding environment. A few examples of ligand effects on Ag clusters are highlighted here, starting with a demonstration by Bakr et al.²⁰ Figure 3b shows that six different aryl-thiol ligands produced similar optical spectra to Ag; however, the ligand with a substitution next to its thiol ($-SH$) group was observed to affect the optical spectrum the most. Using the HSPhF ligand, our group⁴³ quantitatively replaced the ligand shell of $[Ag_{44}(MNBA)_{30}]^{-4}$ clusters while preserving the core (Figure 4). By performing this modification, we



Figure 4. Phase transfer of aqueous $[Ag_{44}(MNBA)_{30}]^{-4}$ clusters into dichloromethane (DCM) using HSPhF as a ligand and tetraphenylphosphonium bromide (TPPB) as a counterion.⁴³ Reprinted from ref 43 with permission.

solubilized the aqueous Ag_{44} clusters into the organic phase and endowed them with luminescence. The report of Bootharaju et al.⁵⁷ revealed reversible tuning of the cluster size and solubility of Ag clusters via ligand effects. These researchers transformed $Ag_{32}(SG)_{19}$ clusters,³⁷ reassigned to $Ag_{35}(SG)_{18}$,⁵⁷ into $[Ag_{44}(SPhF)_{30}]^{-4}$ and vice versa by exploiting the differences in the binding energy of the Ag–S bond arising from different thiol ligands. In addition to tuning the size, other properties, such as chirality, can also be introduced to a cluster via the ligands, as described by Cao et al.⁵⁸ These researchers induced chirality in an achiral Au_{25} cluster by capping it with a chiral ligand, such as (R/S)-2-amino-3-phenylpropane-1-thiol, which could be useful in modern optics. Chirality in Ag clusters has yet to be explored; however, a handful of reports probed chiral-thiol-protected Ag clusters.^{19,59}

Ligands can also select a particular cluster size (especially with Ag) even though the actual mechanism is not yet fully known. This capability presents a rare opportunity to study the properties of clusters of the same core size with various ligands. For example, selenophenol was used to reversibly produce $[Ag_{44}(SePh)_{30}]^{-4}$ clusters.⁶⁰ The oxidation of $[Ag_{44}(SePh)_{30}]^{-4}$ with H_2O_2 produced a Ag(I)–selenolate complex whose successive reduction with $NaBH_4$ yielded the original $[Ag_{44}(SePh)_{30}]^{-4}$ clusters.⁶⁰ This finding demonstrates that the HSePh ligand selects the particular cluster size (Ag_{44}) that

is the most thermodynamically stable among clusters of other sizes. Our recent work using thiols^{43,57} instead of selenols also supports this finding. We examined the size-selection in a different manner; instead of exploiting reductive–oxidative conditions, as performed by the Pradeep group, we used the ligand-exchange method described in Figure 4. Here, aqueous $[Ag_{44}(MNBA)_{30}]^{-4}$ ⁴³ and $Ag_{35}(SG)_{18}$ clusters⁵⁷ were used as starting materials and were then phase transferred into DCM by the HSPhF ligand. Remarkably, after ligand exchange, we obtained the same $[Ag_{44}(SPhF)_{30}]^{-4}$ cluster reported earlier^{20,29} in both cases. These results demonstrated the size-selection by the HSPhF ligand is independent of the original cluster size. It is speculated that the steric effects of the ligands along with the unique synergism of the metal, nature of the ligand, and solvent environment are responsible for the selection of the thermodynamically stable cluster size.

Bidentate and tridentate ligands are also interesting for tuning cluster properties, where simultaneous attachment of the bidentate/tridentate thiol or phosphine groups to a metal core could create a rigidity/strain within a cluster. The use of monodentate aryl-thiols, such as *p*-MBA or HSPhF, is known to produce hollow icosahedral core Ag_{44} clusters,^{28,29} whereas the use of bidentate alkyl-dithiols, such as $NH_4[S_2P(OiPr)_2]$,²⁶ was observed to produce a nonhollow icosahedral-core in a Ag_{21} cluster even though both the clusters contain three-dimensional protecting units. Nevertheless, a fair comparison can be made only with bidentate aryl-dithiols, whose effects on cluster properties have yet to be observed but are also expected to produce nonhollow-core Ag clusters.

Mixed ligand protection also changes the cluster properties. For instance, the use of phosphine in addition to a thiol ligand completely changed the spherical shape of a purely thiolated Au_{25} core³⁵ to a rod shape.^{61,62} This overall shape change led to poor performance of the rod-shaped Au_{25} cluster in catalysis,⁶³ such as the oxidation of styrene and hydrogenation of α,β -unsaturated benzalacetone. By contrast, in the case of Ag, the use of the coligands phosphine⁶⁴ and diphosphine⁶⁵ with the same thiol (HSPhF₂) produced Ag_{14} ⁶⁴ and Ag_{16} ⁶⁵ clusters instead of Ag_{44} ,²⁹ which is expected when the HSPhF₂ ligand is used alone. In the former case, phosphine preserved the Au_{25} core while changing its shape; however, in the latter case, the phosphine roughly preserved the sphericity of the Ag_{44} core²⁹ while shrinking its size. These changes caused by the mixed ligand systems provide an opportunity to study the fundamental changes in the properties of clusters caused by mixed ligands. A theoretical study of the ligand effects on clusters by the Jiang group⁶⁶ revealed that the stronger van der Waals forces and steric effect through a ligand are critical to the cluster stability and other related properties. Yacaman's group⁶⁷

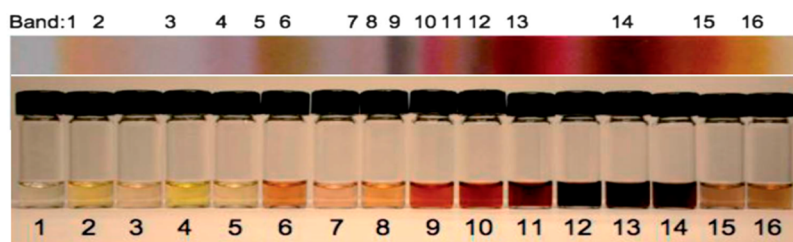


Figure 5. Extracted gel bands of $Ag_m(SG)_n$ clusters (top panel) and their corresponding aqueous solutions (bottom panel). Except for band 6, which is $Ag_{32}(SG)_{19}$, the molecular formula for other bands are not known with atomic precision.⁵¹ Adapted from ref 51 with permission.

Table 1. Selection of Atomically Precise Thiol- and Thiol-Phosphine-Protected Ag Clusters and Their Photophysical Properties

S.N.	chemical formula	excitation (nm)	emission (nm)	characterization	reference
1	Ag ₁₅₂ (PET) ₆₀	375	800	MALDI	69
3	Ag ₄₄ (SPhF) ₃₀	596, 643	1375	single-crystal	29
4	Ag ₃₅ (SG) ₁₈	420, 500	650	ESI-MS	57
5	Ag ₃₂ (SG) ₁₉	420, 500	680	ESI-MS	23
6	Ag ₃₂ (DPPE) ₅ (SPhCF ₃) ₂₄	360	440	single-crystal	65
7	Ag ₂₅ (DHLA) ₁₄	355	680	ESI-MS	81
8	Ag ₁₆ (SG) ₉	489	647	ESI-MS	77
9	Ag ₁₆ (DPPE) ₄ (SPhF ₂) ₁₄	360	440	single-crystal	65
10	Ag ₁₅ (SG) ₁₁	470	665	ESI-MS	22
11	Ag ₁₄ (SPhF ₂) ₁₂ (PPh ₃) ₈	360	536	single-crystal	64
12	Ag ₁₁ (SG) ₇	440	705	ESI-MS	25
13	Ag ₉ (MSA) ₇	625	720	ESI-MS	42
14	Ag ₉ (SG) ₆	379	495	ESI-MS	77
15	Ag ₈ (MSA) ₈	550	650	ESI-MS	24
16	Ag ₇ (MSA) ₇	350	440	ESI-MS	24

also observed that the ligand was one of the key players affecting the cluster absorption properties.

Understanding the Properties of Ag Nanoclusters. Absorption spectroscopy is routinely used in the characterization of organic molecules and organometallic complexes because it can distinguish between different conformers and resonances. Because the number of allowed transitions is constrained by selection rules, absorption spectra can also provide valuable information about the symmetry, band gap, and electronic/geometric structure associated with a particular system. This basic knowledge is also useful for distinguishing metal clusters with different sizes. Several gel-purified magic Au_m(SG)_n clusters³ were first distinguished from each other based on their unique optical spectra, which was confirmed by their mass measurements, thus firmly establishing absorption spectroscopy as the first indispensable diagnostic tool for characterization. Similar work involving differentiating Ag_m(SG)_n clusters (Figure 5)^{4,23,51} was also performed via absorption spectroscopy even though most of these Ag_m(SG)_n clusters await mass characterization, which highlights the importance of absorption spectroscopy in cluster identification. Absorption spectra arise deep within the cluster structure due to the combined effects of the core, ligand, and environment. Some progress in this regard has been made by correlating the experimental absorption spectrum of a [Au₂₅(PET)₁₈]⁻ cluster with its crystal structure in 2008 by Zhu et al.³⁵ via time-dependent (TD) density functional theory (DFT). The appearance of the highly structured optical spectrum of [Au₂₅(PET)₁₈]⁻, unlike the ~525 nm peak of Au plasmons, was attributed to intraband (sp → sp) and interband (d → sp) transitions within the cluster.³⁵ In other words, the transitions arising at the red end of the spectrum are attributed to the metal core, whereas the blue end are dominated by both metal and ligand characteristics, that is, -S-Au-S-Au-S- motifs.³⁵ On the basis of this information, the Aikens group²⁰ predicted the size and crystal structure of IBANs in 2009. Neither the size nor the crystal structure was precisely known at the time; however, these researchers simulated the absorption features of IBANs and predicted a size of 25 atoms (i.e., Ag₂₅).²⁰ Later, mass spectrometry and single-crystal X-ray diffraction measurements proved otherwise, that is, IBANs are Ag₄₄ clusters.^{21,28,29} Although the theoretical prediction using DFT did not match the experimental data for IBANs, it helped the theoretical community tremendously in further refining their predictions, such as in 2010, when

Lopez-Acevedo et al.⁶⁸ predicted the crystal structure of Au₃₈(SR)₂₄ using DFT before the publication of the actual experimental structure.³⁶

Despite some success in deciphering the absorption spectrum of the cluster, significant work lies ahead in predicting the crystal structures and origin of such a spectrum. Determining and predicting the most influencing factors to tune the optical spectra of clusters remains a challenge. Some qualitative studies on tuning the optical spectra of Ag clusters based on the ligand, temperature,²⁰ and core size^{4,51} have been reported previously. Although it remains a daunting task to propose the crystal structure from an optical spectrum of the known mass species, attempts have been pursued to predict the crystal structures^{22,69} for existing and emerging Ag clusters, including doped clusters^{46,47} whose validity awaits actual crystallization of the cluster.

In addition to absorption, clusters also display luminescence behavior, by which it might be possible to predict the cluster size if the emission is due to the bandgap (E_g) transition. This potential was first recognized by Kubo⁷⁰ in 1962 with a simple scaling factor of E_f/N , that is, the energy gap in small metal clusters scales as $1/N$, where N is the total number of atoms, and E_f is the Fermi energy of silver 5.49 eV.^{31,71} The absence of fluorescence in bulk metals is due to overlapping energy states that provide numerous nonradiative pathways for the decay of an excited electron.⁷² However, because of the presence of discrete energy states, small metal clusters exhibit fluorescence.⁷³ Early work by the Whetten group⁷² attributed intra-band (sp → sp) transitions within a metal core to the photoluminescence of <2-nm-sized Au clusters. Subsequent work from the same group on the precise cluster Au₂₈(SG)₁₆^{5,74} later corrected to Au₂₅(SG)₁₈³ provided similar arguments for the fluorescence/phosphorescence albeit with some implications of the ligand effects.⁷⁴ While studying the fluorescent properties of Au clusters, Zheng et al.⁷⁵ (Knight et al.⁸ for bare Na_n clusters) empirically established a scaling factor of $E_f/N^{1/3}$ between the energy gap and the number of atoms in ligand-protected metal clusters based on the Jellium model. The Zheng et al.⁷⁵ relation was effective up to 20-atom Au clusters, beyond which correction factors were needed to explain the emission and cluster-size relationship.

In favor of Ag clusters, the Dickson group⁷⁶ first reported fluorescent Ag clusters encapsulated by dendrimers. Huang and Murray's¹⁸ work pointed to the interband recombination

(between d and sp) as a fluorescence source for Ag clusters. Although the exact origin of the fluorescence in precise Ag clusters remains disputable, Cathcart et al.¹⁹ and Bakr et al.^{20,21} reported additional luminescence Ag clusters protected by glutathione, cysteine, and aryl-thiols. It is logical to assume that the visible luminescence from a relatively small-size cluster will be blue-shifted compared with a large cluster because the HOMO–LUMO gap changes with the size. However, counter-intuitive observations (see Table 1), such as visible luminescence from a large Ag_{152} ⁶⁹ cluster compared with small IR-luminescence $[\text{Ag}_{44}(\text{SPhF})_{30}]^{-4}$ ²⁰ cluster and a blue shift in the luminescences of $\text{Ag}_9(\text{SG})_6$ ⁷⁷ and $\text{Ag}_{15}(\text{SG})_{11}$ ²² compared with those of $\text{Ag}_8(\text{MSA})_8$ ²⁴ and $\text{Ag}_{11}(\text{SG})_7$,²⁵ add some other parameters that affect the cluster-size and emission relationship. These luminescence-altering factors can be due ligand and surface state transitions, in addition to contributions from the cluster's surrounding environment. For example, Li et al.⁷⁸ and Xu et al.⁵⁵ demonstrated the luminescence change by understanding the temperature effects on precise Ag clusters, whereas Díez et al.⁵⁶ observed that the solvent rather than the size affected the emission. Recent work from the Jin group⁷⁹ on Au clusters emphasized the ligand, as they discovered that ligand → metal charge transfer (LMCT) either via the Au–S bond or through the electron-rich atoms/groups (e.g., N, O, –COOH, –NH₂) was responsible for the fluorescence. Similar LMCT in Ag clusters was observed by Pelton et al.⁸⁰ while studying transient-absorption spectroscopy of IBANs. A summary of the photophysical properties associated with some of the precise Ag clusters with their characterization techniques is provided in Table 1.

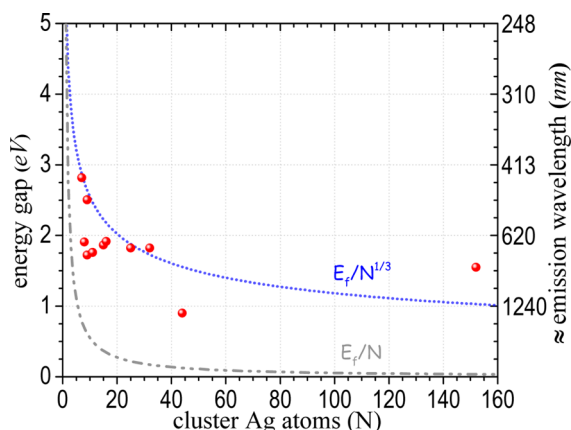


Figure 6. Correlation of the emission energy of Ag cluster size as predicted by Kubo (gray, E_f/N) and Zheng et al. (blue, $E_f/N^{1/3}$) scaling factors. The red spheres represent the actual emission energy of the thiolated Ag clusters.

The luminescence data in Table 1 of Ag clusters were analyzed using the scaling factors reported by Kubo⁷⁰ and Zheng et al.⁷⁵ (Figure 6) to study the size-dependent emission properties. Both the Kubo and the Zheng et al. models are found to be unsuitable for explaining the entire data and therefore are unable to predict the relationship between size and emission of Ag clusters. However, unlike Au where the model of Zheng et al. is somewhat reasonable,⁷⁵ significant deviation is observed in Ag clusters in the size range of ~8–15 and ≥ 44 atoms. The actual origin of such discrepancy is a complex problem with many potential variables and assumptions and is beyond the scope of this article; nevertheless, it can be understood that the photoluminescence may not originate only

from the band gap of clusters, which limits our ability to predict Ag cluster size spectroscopically with the emission energy versus E_g relation.

Also, when discussing spectroscopic properties related to Ag clusters, caution should be exercised because Ag is prone to oxidation and is sensitive to light. Relatively few Ag clusters are reported (Table 1), and some might be impure and unstable.⁶⁹ Trace impurities in Ag cluster samples with other sizes, especially the luminescent ones arising from oxidation or other processes from the existing clusters during spectroscopic measurements, could significantly affect emission spectrum. This effect adds uncertainty to the interpretation of the data and therefore should be considered prior to estimation of Ag cluster size via emission $\propto E_g$ relation.

In order to minimize the decomposition of Ag clusters with light in optical spectroscopy and to identify materials close to their native states, mass spectrometry (MS) with softer ionization method is essential. The Whetten group used laser desorption ionization (LDI) MS for the characterization of Au clusters.^{5,6,17} However, because of the significant fragmentations from the LDI, relatively softer techniques with high resolution, such as matrix-assisted laser desorption ionization (MALDI) and electrospray ionization (ESI), are more prevalent today. The ESI MS, in particular, is preferred over MALDI because it neither uses light (laser) nor a solidified sample with matrix. The Tsukuda³ and Griffith groups²³ characterized magic-size $\text{Au}_m(\text{SG})_n$ and $\text{Ag}_{32}(\text{SG})_{19}$ clusters, respectively, using ESI MS. The Griffith group observed that the Ag thiolates were more fragile and prone to fragmentation than their Au counterparts.²³ Nevertheless, MS is one of the most important tools for the characterization of clusters where the molecular formula of the compound of interest is important for identification and crystallization poses a significant challenge.

Crystallization ensures purity of the material by consolidating molecules in a dense space where single-crystal X-ray diffraction can reveal the ultimate atomic coordinates in 3D space. Detection of the intact cluster or its fragments in MS sometimes make interpreting a mass spectrum quite challenging because several processes, such as rearrangement, coordination, and fragmentation, occur in parallel in the gas phase. Most of these gas-phase metal clusters are difficult to crystallize or manipulate because they either change their properties or lose identity when they contact other species. Growing a single crystal from the solution phase of the cluster could be a possibility, although crystallization is challenging. Despite these challenges, there are reports of the crystallization of pure-thiol and mixed-ligand Ag clusters.^{28,29,64,65}

Similar to molecules, clusters prefer certain types of crystal habits. For example, graphite and diamond are composed of the same carbon building blocks; however, their respective crystal habits are completely different, that is, tabular and octahedral. This tunability of the crystal habit results in new properties for materials. A recent report by Yao et al.⁸² brings this promise to the cluster community, as shown in Figure 7. These researchers were able to perform a crystal habit transition from a rhombohedral to an octahedral state for the same $[\text{Ag}_{44}(p\text{-MBA})_{30}]^{-4}$ system by swapping counterions.⁸² In this case, the directionality provided by the counterions H^+ via H-bonding was disrupted with Cs^+ ions, which led to the change in the crystal habit. The ability to swap counterions with other metalations, such as Ca^{2+} and Al^{3+} , would allow engineers to construct new 3D shapes using $[\text{Ag}_{44}(\text{SR})_{44}]^{-4}$ as building blocks

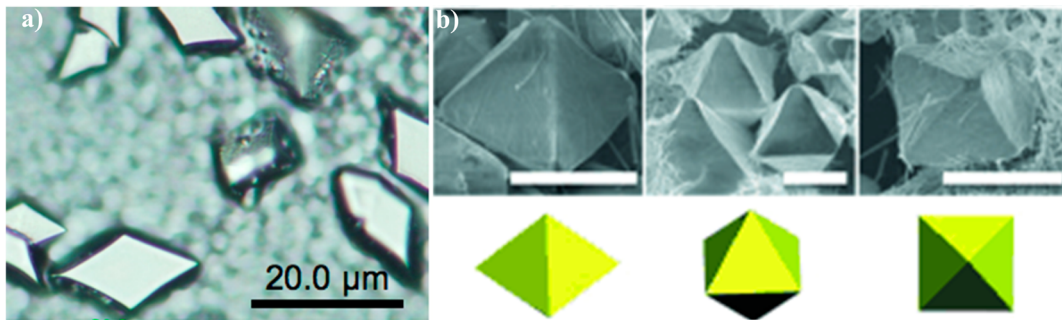


Figure 7. Crystals of $[\text{Ag}_{44}(p\text{-MBA})_{30}]^{-4}$ clusters (a) with a rhombus shape crystallized from a dimethylformamide (DMF) solution with a completely protonated ligand as observed under an optical microscope²⁸ and (b) electron micrograph of the octahedron-shaped crystals grown from dimethyl sulfoxide (DMSO)/water using Cs^+ counterions⁸² (scale bar = 10 μm). Adapted from refs 28 and 82 with permission.

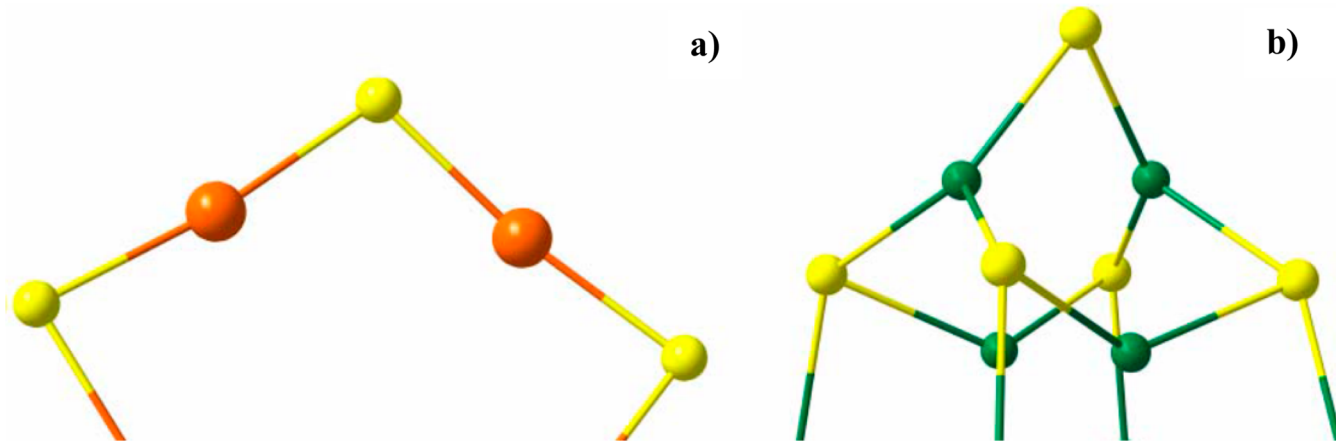


Figure 8. Structure of the cluster-protecting motifs Au_2S_3 (left) and Ag_2S_5 (right) observed in Au and Ag clusters, respectively.^{28,29,35} Color legend of spheres: Au, orange; Ag, green; and S, yellow. Adapted from ref²⁹ with permission.

in the future, which could result in dramatically useful properties at the macroscale that have already been achieved at the microscale.^{28,82}

Manifestation of fundamental properties such as the optical activity and reactivity is key to understanding metal clusters better and can ultimately be achieved using single-crystal X-ray diffraction for both aqueous²⁸ and organic²⁹ soluble Ag clusters. Surprisingly, single-crystal X-ray diffraction revealed a completely different protecting layer for Ag clusters than for Au clusters, where mono ($-\text{S}-\text{Au}-\text{S}-$) and dimeric ($-\text{S}-\text{Au}-\text{S}-\text{Au}-\text{S}-$) motifs were predominant (Figure 8).^{35,36}

As observed in Figure 8, the Au clusters are protected with one-dimensional motifs whereas the Ag clusters crystallized so far are protected with three-dimensional motifs. Although the ubiquitous nature of the three-dimensional Ag_2S_5 motif has yet to be proven, it can be argued that the many one-dimensional motifs would provide better coverage for a cluster core than the three-dimensional motif. This hypothesis is also supported by the fact that $[\text{Ag}_{44}(p\text{-MBA})_{30}]^{-4}$ contains ~50% void space²⁸ in the crystal volume, making it highly affected by its surrounding, which could explain the relatively low stability of Ag clusters compared with Au clusters. In stark contrast, our observations of year-long ambient stability in other Ag clusters, such as aqueous $[\text{Ag}_{44}(\text{MNBA})_{30}]^{-4}$ ⁴⁸ and $\text{Ag}_{35}(\text{SG})_{18}$ ⁵⁷ clearly indicate the opposite physicochemical behavior.

Perspectives. The syntheses of Ag clusters involve multistep and hours-long processes^{20,29} with few exceptions.²⁸ For instance, the synthesis of $[\text{Ag}_{44}(\text{SR})_{30}]^{-4}$ requires days based on the protocol of Bakr et al.,²⁰ whereas a similar composition can be

obtained in a one-pot synthesis in an hour using the procedure described by Desiréddy et al.²⁸ This shortening of the synthesis time is crucial for materials processing and applications on industrial scales. Nevertheless, the key factors behind this drastic reduction in synthesis time have not been seriously considered. In addition, in $\text{Ag}_m(\text{SG})_n$ clusters, what factors determine the values of m and n remains a mystery both experimentally and theoretically and therefore require attention.

For tuning the size of Ag clusters, researchers should look at those aryl thiols that have substitution adjacent to the thiol group. This subtle change in ligands could unlock the key to producing Ag clusters of different sizes.

Silver has received less attention than has gold from the beginning even though it is inexpensive. This inferiority of silver over gold was due to its susceptibility to oxidation. However, at the nanoscale, Ag is not as susceptible to oxidation as indicated by the resistance of some Ag clusters, such as $\text{Ag}_{35}(\text{SG})_{18}$ ⁵⁷ and $[\text{Ag}_{44}(\text{MNBA})_{30}]^{-4}$.⁴⁸ Many magic clusters in the $\text{Au}_m(\text{SG})_n$ family³ have been successfully characterized with atomic precision because they are stable. Years have passed

since the isolation of 20+ magic $\text{Ag}_m(\text{SG})_n$ clusters;⁴ however, few^{22,23} of these clusters have been characterized. This lack of progress in the characterization of Ag clusters lies in either cluster stability or instrumental limitations. Stability appears to be a critical factor despite the significant technical know-how acquired from the characterization of analogous $\text{Au}_m(\text{SG})_n$ clusters because the instability associated with Ag clusters can ruin a sample, as decayed products accumulate over time, resulting in poor data and confusion. For example, four research groups independently working on the same glutathione Ag system detected $\text{Ag}_m(\text{SG})_n$ species with very similar absorption features that were assigned as $\text{Ag}_{35}(\text{SG})_{18}$,⁵⁷ $\text{Ag}_{32}(\text{SG})_{19}$,²³ $\text{Ag}_{31}(\text{SG})_{19}$,²² and $\text{Ag}_{16}(\text{SG})_9$.⁷⁷

Although some clues for improving the stability of Ag clusters were revealed from a single-crystal structure of Ag_{44} ,^{28,29} and other Ag species,^{64,65} significant work needs to be performed before actual manipulation of the Ag cluster stability can be achieved. Among all available Ag species,^{20,28,29,48} aqueous $[\text{Ag}_{44}(\text{MNBA})_{30}]^{-4}$ is observed to be the most stable with an 18-electron core. However, this cluster undergoes rapid ligand exchange with different aryl-thiols in a matter of seconds, producing less-stable species, such as $[\text{Ag}_{44}(\text{SPhF})_{30}]^{-4}$ and $[\text{Ag}_{44}(2\text{-naphthalenethiol})_{30}]^{-4}$ with a Ag_{44} core intact.⁴³ A question remains unanswered: Why would the cluster sacrifice its stability to migrate into a less-stable state? Arguments that an excess ligand pushes the equilibrium in favor of the ligand exchange are reasonable. However, reversibility was not observed when excess MNBA ligand was used to obtain the original $[\text{Ag}_{44}(\text{MNBA})_{30}]^{-4}$ from the $[\text{Ag}_{44}(\text{SPhF})_{30}]^{-4}$ clusters in our experiments.

In addition, unlike Au, where the same ligand PET can produce different size $\text{Au}_m(\text{PET})_n$ clusters,⁷ Ag is known to form the same Ag_{44} cluster with different aryl thiols.^{20,43} This limits our ability to diversify cluster size; however, a subtle yet important empirical factor for cluster size tuning is often lost. For tuning the size of Ag clusters, researchers should look at those aryl thiols that have substitution adjacent to the thiol group. This subtle change in ligands could unlock the key to producing Ag clusters of different sizes, which needs to be considered.

Another concern is the superatom theory. The electronic and geometric shell closure ideas of the superatom theory represent significant theoretical advancements in explaining the stability associated with clusters. However, some clusters do not have closed structures (Figure 9), do not obey superatom theory, but are very stable. Therefore, the superatom theory requires modification to include clusters with open shells. Moreover, having a closed electronic shell does not guarantee that the cluster is a superatom even though it is one criterion. For example, the $[\text{Au}_{23}(\text{SC}_6\text{H}_{11})_{16}]^-$ cluster^{7,83} has an 8e^- core, analogous to the $[\text{Au}_{25}(\text{PET})_{18}]^-$ cluster; however, DFT analysis based on the experimental crystal structure proved that this cluster was not a superatom. In this case, where the superatom theory has a limited use, Clemenger³⁸ suggested that the clusters would undergo distortion to lower their energies; however, a concrete theory is not available yet. Thus, we should be cautious regarding the superatom theory. Deeper understanding may imply that it is feasible in principle to synthesize arbitrary Ag_m clusters (where $m = 1, 2, 3, 4, \dots$) although these clusters may vary in the stability. In the future, we could have numerous Ag_m clusters with various properties that could go beyond the periodic table of elements to meet our needs. We

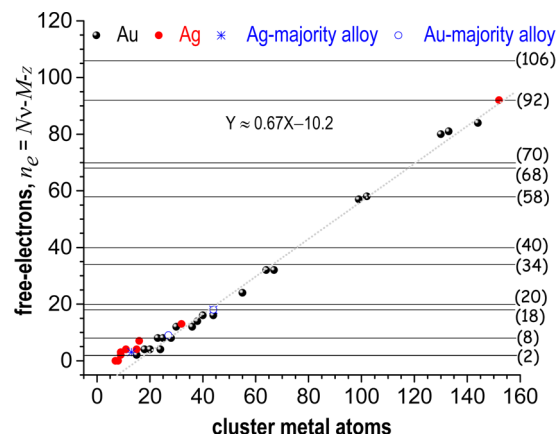


Figure 9. Stability belt of ligand-protected metal clusters obtained after analysis of the free electrons present in the thiol-protected Ag_mL_n and Au_mL_n and their alloys. The numbers inside the parentheses indicate electron-shell closure, and the dotted line is the actual fit to Au_mL_n clusters with a slope of $\approx 2/3$ (data compiled from Table 1 and refs 7, 49, 53, 29, and 84).

believe that emerging Ag clusters may follow a particular trend described by the stability curve presented in Figure 9.

It is apparent from Figure 9 that ligand-protected metal clusters follow a certain trend described by the plot of n_e versus cluster metal atoms. Notably, the clusters populate themselves around a line with a slope of $2/3$. Therefore, the magic size clusters maintain a magic ratio of approximately two free electrons for every three metal atoms with some intercept value (Figure 9). We expect that emerging Ag clusters would follow the trend described by the stability curve because it would be difficult to synthesize monothiol protected clusters that deviate considerably from the projection of the stability curve. We also studied the plot of $(n_e - |z|)$ versus cluster core atoms (not shown) but did not find much difference because the majority of clusters are neutral. Regardless of the superatom theory, this stability curve can serve as a guide for predicting the sizes of Ag_m clusters that can be synthesized, systematized, and could be studied like the periodic table of elements. Furthermore, the stability curve also suggests a threshold of a cluster size of ~ 15 atoms, beyond which the core atom count in a cluster would always be greater than the ligand count.

Magic size clusters maintain a magic ratio of approximately two free electrons for every three metal atoms with some intercept.

Finally, impending chaos is on the horizon for the systematic study and organization of existing and emerging ligand-protected metal clusters. Therefore, a healthy debate on this matter is expected in the scientific community. Attempts toward the systematic study of bare gas-phase metal clusters in a 3D periodic table have been discussed in the literature;^{85,86} however, this effort has not been made for ligand-protected metal clusters. Our views in this regard are presented below.

Natural elements are arranged in the standard form of the periodic table as a function of their increasing atomic numbers such that no two elements have the same position in the 7×18 grid table (Figure 10, top panel). However, the arrangement of clusters is different; these structures possess a few hundred

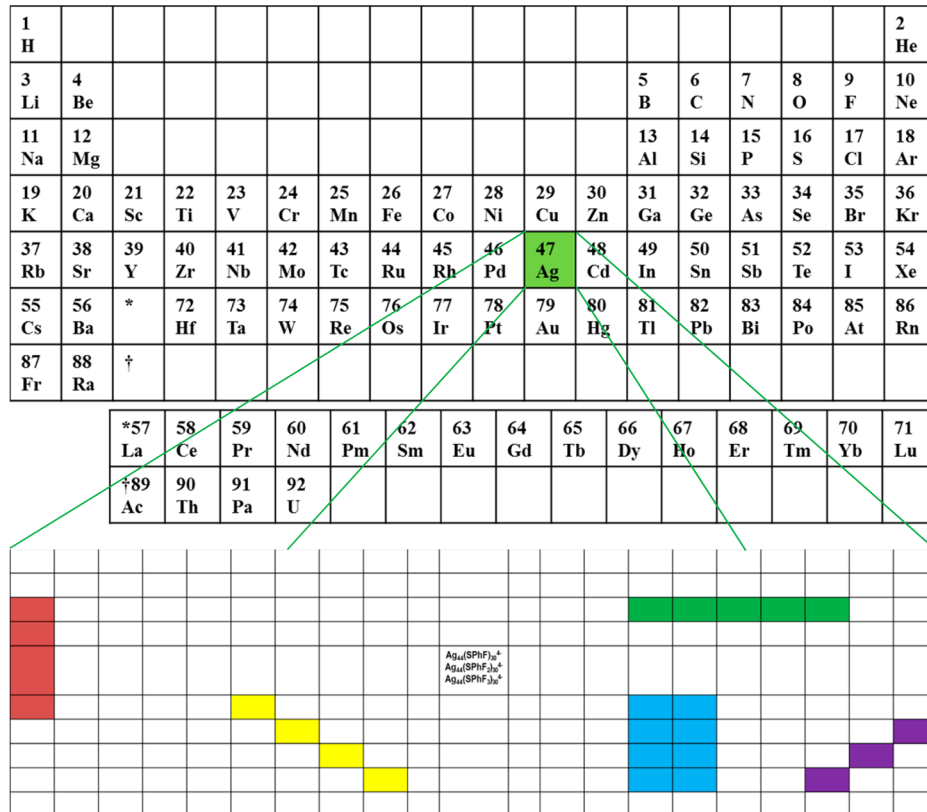


Figure 10. Elemental periodic table (top) along with a proposed clusterograph of Ag clusters (bottom). The yellow, green, red, blue, and violet shading highlights the similarities in the properties of different Ag clusters at the local or regional levels.

atoms clinging together, resulting in an additional dimension that is not needed for atoms. Moreover, existing and emerging clusters would easily outnumber the total elements by a large margin, thus complicating their systematic study, given the number of ways that atoms can be arranged in a 3D cluster space.

Nevertheless, placing Ag_mL_n clusters in a periodic table similar to Mendeleev's is an option. However, finding a reasonable basis for the arrangement of clusters in the most meaningful manner is challenging. We have many candidates for bases: the total atomic number or weight, cluster electron configuration, cluster energy, electronegativity, length, so forth. Using the total atomic number or weight as a basis, which is obtained by summing the contributions from all the atoms present in a cluster, appears unsuitable because it would produce a very large number. Superatom/cluster electronic configuration, that is, categorizing clusters into S, P, D, F, G, ... blocks is possible; however, some clusters do not follow the superatom theory. The exclusion of nonsuperatoms or superatoms with zero free electrons or in a negative state (i.e., the case of a greater ligand than metal count) could be a serious problem in this case. An arrangement based on either the total energy or electronegativity of a cluster is less likely because of the fractional numbers and the high probability of similar values for many different clusters. Arranging clusters according to their length is promising because the nanoscale properties depend on the length scale. However, defining a precise length is difficult because of the variability in cluster shapes. Therefore, we think that organizing clusters based on the core metal atom count would simplify the task as we can have very precise numbers 1, 2, 3, 4, 5, ... similar to the atomic numbers in the periodic table

of elements. Depending on the shape, size, and cluster properties, we do expect the same-size clusters to be assigned to a single or multiple cells. However, the length and width of the periodic table for Ag_mL_n clusters currently remain changeable due to inadequate data.

Despite these issues, the question arises of how the periodic table of clusters would look when they are arranged as a function of increasing core atoms. Certainly, it would be much different from the periodic table of elements (Figure 10, top panel). Unlike the periodic table of elements, periodicity will be lost with clusters. Therefore, the future periodic table of clusters would look like a megapixel photograph, where a pixel would represent either a superatom or a nonsuperatom cluster. This photograph of clusters (abbreviated here as "clusterograph") would have local or regional similarities among different clusters across the entire grid (highlighted in red, yellow, green, blue, and violet) but no recurring periodicity. Furthermore, in contrast to the periodic table of elements, similar superatom clusters, such as [Ag₄₄(SPhF)₃₀]⁻⁴, [Ag₄₄(SPhF₂)₃₀]⁻⁴, and [Ag₄₄(SPhF₃)₃₀]⁻⁴, would be given a single cell even though each cluster contains a different ligand. We believe that most elements in the periodic table of elements such as Cu, Au, Pd, and Pt would have their own clusterograph as we demonstrate here for Ag in Figure 10, bottom panel. Interpreting these clusterographs would be more appropriate for computers than for humans.

■ AUTHOR INFORMATION

Corresponding Author

*E-mail: osman.bakr@kaust.edu.sa.

Notes

The authors declare no competing financial interest.

Biographies

Chakra P. Joshi is currently working at the KAUST Functional Nanomaterials Lab. His research interests include Ag cluster syntheses and their characterization.

Megalamane S. Bootharaju is currently pursuing his postdoctoral study at the KAUST Functional Nanomaterials Lab. His main research interests include investigating the ligand exchange of metal clusters both theoretically and experimentally.

Osman M. Bakr is currently working as an associate professor of materials science and engineering at KAUST. His broad research interests include the fabrication, characterization, and photovoltaic applications of nanomaterials. For further information about the research work in Dr. Bakr's lab, please visit <http://funl.kaust.edu.sa/Pages/Home.aspx>.

ACKNOWLEDGMENTS

The authors acknowledge funding from King Abdullah University of Science and Technology (KAUST).

REFERENCES

- (1) Feynman, R. P. There is Plenty of Room at the Bottom. *Caltech Eng. Sci.* **1960**, *23*, 22–36.
- (2) Becker, E. W.; Bier, K.; Henkes, W. Strahlen aus kondensierten Atomen und Molekülen im Hochvakuum. *Eur. Phys. J. A* **1956**, *146*, 333–338.
- (3) Negishi, Y.; Nobusada, K.; Tsukuda, T. Glutathione-Protected Gold Clusters Revisited: Bridging the Gap between Gold(I)–Thiolate Complexes and Thiolate-Protected Gold Nanocrystals. *J. Am. Chem. Soc.* **2005**, *127*, 5261–5270.
- (4) Kumar, S.; Bolan, M. D.; Bigioni, T. P. Glutathione-Stabilized Magic-Number Silver Cluster Compounds. *J. Am. Chem. Soc.* **2010**, *132*, 13141–13143.
- (5) Schaaff, T. G.; Knight, G.; Shafiqullin, M. N.; Borkman, R. F.; Whetten, R. L. Isolation and Selected Properties of a 10.4 kDa Gold:Glutathione Cluster Compound. *J. Phys. Chem. B* **1998**, *102*, 10643–10646.
- (6) Price, R. C.; Whetten, R. L. All-Aromatic, Nanometer-Scale, Gold-Cluster Thiolate Complexes. *J. Am. Chem. Soc.* **2005**, *127*, 13750–13751.
- (7) Jin, R. Atomically Precise Metal Nanoclusters: Stable Sizes and Optical Properties. *Nanoscale* **2015**, *7*, 1549–1565.
- (8) Knight, W.; Clemenger, K.; de Heer, W.; Saunders, W.; Chou, M.; Cohen, M. Electronic Shell Structure and Abundances of Sodium Clusters. *Phys. Rev. Lett.* **1984**, *52*, 2141–2143.
- (9) Kroto, H. W.; Heath, J. R.; O'Brien, S. C.; Curl, R. F.; Smalley, R. E. C60: Buckminsterfullerene. *Nature* **1985**, *318*, 162–163.
- (10) Jin, R.; Cao, Y.; Mirkin, C. A.; Kelly, K. L.; Schatz, G. C.; Zheng, J. G. Photoinduced Conversion of Silver Nanospheres to Nanoprisms. *Science* **2001**, *294*, 1901–1903.
- (11) Eustis, S.; El-Sayed, M. A. Why Gold Nanoparticles are More Precious than Pretty Gold: Noble Metal Surface Plasmon Resonance and its Enhancement of the Radiative and Nonradiative Properties of Nanocrystals of Different Shapes. *Chem. Soc. Rev.* **2006**, *35*, 209–217.
- (12) Faraday, M. The Bakerian Lecture: Experimental Relations of Gold (and Other Metals) to Light. *Philos. Trans. R. Soc. London* **1857**, *147*, 145–181.
- (13) Turkevich, J.; Stevenson, P. C.; Hillier, J. A Study of the Nucleation and Growth Processes in the Synthesis of Colloidal Gold. *Discuss. Faraday Soc.* **1951**, *11*, 55–75.
- (14) McPartlin, M.; Mason, R.; Malatesta, L. Novel Cluster Complexes of Gold(0)-gold(I). *J. Chem. Soc. D* **1969**, 334–334.
- (15) Gutrat, B. S.; Englert, U.; Wang, Y.; Simon, U. A Missing Link in Undecagold Cluster Chemistry: Single-Crystal X-ray Analysis of $[Au_{11}(PPh_3)_7Cl_3]$. *Eur. J. Inorg. Chem.* **2013**, *2013*, 2002–2006.
- (16) Brust, M.; Walker, M.; Bethell, D.; Schiffen, D. J.; Whyman, R. Synthesis of Thiol-derivatised Gold Nanoparticles in a Two-phase Liquid-Liquid System. *J. Chem. Soc., Chem. Commun.* **1994**, 801–802.
- (17) Schaaff, T. G.; Shafiqullin, M. N.; Khouri, J. T.; Vezmar, I.; Whetten, R. L. Properties of a Ubiquitous 29 kDa Au:S R Cluster Compound. *J. Phys. Chem. B* **2001**, *105*, 8785–8796.
- (18) Huang, T.; Murray, R. W. Luminescence of Tiopronin Monolayer-Protected Silver Clusters Changes To That of Gold Clusters upon Galvanic Core Metal Exchange. *J. Phys. Chem. B* **2003**, *107*, 7434–7440.
- (19) Cathcart, N.; Mistry, P.; Makra, C.; Pietrobon, B.; Coombs, N.; Jelokhani-Niaraki, M.; Kitaev, V. Chiral Thiol-Stabilized Silver Nanoclusters with Well-Resolved Optical Transitions Synthesized by a Facile Etching Procedure in Aqueous Solutions. *Langmuir* **2009**, *25*, 5840–5846.
- (20) Bakr, O. M.; Amendola, V.; Aikens, C. M.; Wenseleers, W.; Li, R.; Dal Negro, L.; Schatz, G. C.; Stellacci, F. Silver Nanoparticles with Broad Multiband Linear Optical Absorption. *Angew. Chem. Int. Ed.* **2009**, *121*, 6035–6040.
- (21) Harkness, K. M.; Tang, Y.; Dass, A.; Pan, J.; Kothalawala, N.; Reddy, V. J.; Cliffel, D. E.; Demeler, B.; Stellacci, F.; Bakr, O. M.; McLean, J. A. $Ag_{44}(SR)_{30}^+$: A Silver-Thiolate Superatom Complex. *Nanoscale* **2012**, *4*, 4269–4274.
- (22) Bertorelle, F.; Hamouda, R.; Rayane, D.; Broyer, M.; Antoine, R.; Dugourd, P.; Gell, L.; Kulesza, A.; Mitric, R.; Bonacic-Koutecky, V. Synthesis, Characterization and Optical Properties of low Nuclearity Liganded Silver Clusters: $Ag_{31}(SG)_{19}$ and $Ag_{15}(SG)_{11}$. *Nanoscale* **2013**, *5*, 5637–5643.
- (23) Guo, J.; Kumar, S.; Bolan, M.; Desiraju, A.; Bigioni, T. P.; Griffith, W. P. Mass Spectrometric Identification of Silver Nanoparticles: The Case of $Ag_{32}(SG)_{19}$. *Anal. Chem.* **2012**, *84*, 5304–5308.
- (24) Udaya Bhaskara Rao, T.; Pradeep, T. Luminescent Ag_7 and Ag_8 Clusters by Interfacial Synthesis. *Angew. Chem., Int. Ed.* **2010**, *49*, 3925–3929.
- (25) Baksi, A.; Bootharaju, M. S.; Chen, X.; Häkkinen, H.; Pradeep, T. $Ag_{11}(SG)_7$: A New Cluster Identified by Mass Spectrometry and Optical Spectroscopy. *J. Phys. Chem. C* **2014**, *118*, 21722–21729.
- (26) Dhayal, R. S.; Liao, J.-H.; Liu, Y.-C.; Chiang, M.-H.; Kahalal, S.; Saillard, J.-Y.; Liu, C. W. $[Ag_{21}\{S_2P(OiPr)_2\}_{12}]^+$: An Eight-Electron Superatom. *Angew. Chem. Int. Ed.* **2015**, *54*, 3702–3706.
- (27) Jadzinsky, P. D.; Calero, G.; Ackerson, C. J.; Bushnell, D. A.; Kornberg, R. D. Structure of a Thiol Monolayer-Protected Gold Nanoparticle at 1.1 Å Resolution. *Science* **2007**, *318*, 430–433.
- (28) Desiraju, A.; Conn, B. E.; Guo, J.; Yoon, B.; Barnett, R. N.; Monahan, B. M.; Kirschbaum, K.; Griffith, W. P.; Whetten, R. L.; Landman, U.; Bigioni, T. P. Ultrastable Silver Nanoparticles. *Nature* **2013**, *501*, 399–402.
- (29) Yang, H.; Wang, Y.; Huang, H.; Gell, L.; Lehtovaara, L.; Malola, S.; Häkkinen, H.; Zheng, N. All-Thiol-Stabilized Ag_{44} and $Ag_{12}Ag_{32}$ Nanoparticles with Single-Crystal Structures. *Nat. Commun.* **2013**, *4*, 2422.
- (30) Martins, J. L.; Car, R.; Buttet, J. Variational Spherical Model of Small Metallic Particles. *Surf. Sci.* **1981**, *106*, 265–271.
- (31) de Heer, W. A. The Physics of Simple Metal Clusters: Experimental Aspects and Simple Models. *Rev. Mod. Phys.* **1993**, *65*, 611–676.
- (32) Roach, P. J.; Woodward, W. H.; Castleman, A. W.; Reber, A. C.; Khanna, S. N. Complementary Active Sites Cause Size-Selective Reactivity of Aluminum Cluster Anions with Water. *Science* **2009**, *323*, 492–495.
- (33) Walter, M.; Akola, J.; Lopez-Acevedo, O.; Jadzinsky, P. D.; Calero, G.; Ackerson, C. J.; Whetten, R. L.; Grönbeck, H.; Häkkinen, H. A Unified View of Ligand-Protected Gold Clusters as Superatom Complexes. *Proc. Natl. Acad. Sci. U. S. A.* **2008**, *105*, 9157–9162.

- (34) Leuchtner, R. E.; Harms, A. C.; Castleman, A. W. Thermal Metal Cluster Anion Reactions: Behavior of Aluminum Clusters with Oxygen. *J. Chem. Phys.* **1989**, *91*, 2753–2754.
- (35) Zhu, M.; Aikens, C. M.; Hollander, F. J.; Schatz, G. C.; Jin, R. Correlating the Crystal Structure of A Thiol-Protected Au_{25} Cluster and Optical Properties. *J. Am. Chem. Soc.* **2008**, *130*, 5883–5885.
- (36) Qian, H.; Eckenhoff, W. T.; Zhu, Y.; Pintauer, T.; Jin, R. Total Structure Determination of Thiolate-Protected Au_{38} Nanoparticles. *J. Am. Chem. Soc.* **2010**, *132*, 8280–8281.
- (37) Udayabhaskararao, T.; Bootharaju, M. S.; Pradeep, T. Thiolate-Protected Ag_{32} Clusters: Mass Spectral Studies of Composition and Insights into the Ag-Thiolate Structure from NMR. *Nanoscale* **2013**, *5*, 9404–9411.
- (38) Clemenger, K. Ellipsoidal Shell Structure in Free-electron Metal Clusters. *Phys. Rev. B: Condens. Matter Mater. Phys.* **1985**, *32*, 1359–1362.
- (39) Mackay, A. A Dense Non-crystallographic Packing of Equal Spheres. *Acta Crystallogr.* **1962**, *15*, 916–918.
- (40) Luo, Z.; Gamboa, G. U.; Smith, J. C.; Reber, A. C.; Reveles, J. U.; Khanna, S. N.; Castleman, A. W. Spin Accommodation and Reactivity of Silver Clusters with Oxygen: The Enhanced Stability of Ag_{13}^- . *J. Am. Chem. Soc.* **2012**, *134*, 18973–18978.
- (41) Martin, T. P. Shells of Atoms. *Phys. Rep.* **1996**, *273*, 199–241.
- (42) Rao, T. U. B.; Nataraju, B.; Pradeep, T. Ag_9 Quantum Cluster through a Solid-State Route. *J. Am. Chem. Soc.* **2010**, *132*, 16304–16307.
- (43) AbdulHalim, L. G.; Kothalawala, N.; Sinatra, L.; Dass, A.; Bakr, O. M. Neat and Complete: Thiolate-Ligand Exchange on a Silver Molecular Nanoparticle. *J. Am. Chem. Soc.* **2014**, *136*, 15865–15868.
- (44) Choi, J.-P.; Fields-Zinna, C. A.; Stiles, R. L.; Balasubramanian, R.; Douglas, A. D.; Crowe, M. C.; Murray, R. W. Reactivity of $[\text{Au}_{25}(\text{SCH}_2\text{CH}_2\text{Ph})_{18}]^{1-}$ Nanoparticles with Metal Ions. *J. Phys. Chem. C* **2010**, *114*, 15890–15896.
- (45) Sarkar, S.; Chakraborty, I.; Panwar, M. K.; Pradeep, T. Isolation and Tandem Mass Spectrometric Identification of a Stable Monolayer Protected Silver–Palladium Alloy Cluster. *J. Phys. Chem. Lett.* **2014**, *5*, 3757–3762.
- (46) Biltek, S. R.; Mandal, S.; Sen, A.; Reber, A. C.; Pedicini, A. F.; Khanna, S. N. Synthesis and Structural Characterization of an Atom-Precise Bimetallic Nanocluster, $\text{Ag}_4\text{Ni}_2(\text{DMSA})_4$. *J. Am. Chem. Soc.* **2012**, *135*, 26–29.
- (47) Biltek, S. R.; Sen, A.; Pedicini, A. F.; Reber, A. C.; Khanna, S. N. Isolation and Structural Characterization of a Silver–Platinum Nanocluster, $\text{Ag}_4\text{Pt}_2(\text{DMSA})_4$. *J. Phys. Chem. A* **2014**, *118*, 8314–8319.
- (48) AbdulHalim, L. G.; Ashraf, S.; Katsiev, K.; Kirmani, A. R.; Kothalawala, N.; Anjum, D. H.; Abbas, S.; Amassian, A.; Stellacci, F.; Dass, A.; Hussain, I.; Bakr, O. M. A Scalable Synthesis of Highly Stable and Water Dispersible $\text{Ag}_{44}(\text{SR})_{30}$ Nanoclusters. *J. Mater. Chem. A* **2013**, *1*, 10148–10154.
- (49) Yao, C.; Chen, J.; Li, M.-B.; Liu, L.; Yang, J.; Wu, Z. Adding Two Active Silver Atoms on Au_{25} Nanoparticle. *Nano Lett.* **2015**, *15*, 1281–1287.
- (50) Chen, W.-T.; Hsu, Y.-J.; Kamat, P. V. Realizing Visible Photoactivity of Metal Nanoparticles: Excited-State Behavior and Electron-Transfer Properties of Silver (Ag_8) Clusters. *J. Phys. Chem. Lett.* **2012**, *3*, 2493–2499.
- (51) Desiréddy, A.; Kumar, S.; Guo, J.; Bolan, M. D.; Griffith, W. P.; Bigioni, T. P. Temporal Stability of Magic-Number Metal Clusters: Beyond the Shell Closing Model. *Nanoscale* **2013**, *5*, 2036–2044.
- (52) Kumara, C.; Aikens, C. M.; Dass, A. X-ray Crystal Structure and Theoretical Analysis of $\text{Au}_{25-x}\text{Ag}_x(\text{SCH}_2\text{CH}_2\text{Ph})_{18}^-$ Alloy. *J. Phys. Chem. Lett.* **2014**, *5*, 461–466.
- (53) Udayabhaskararao, T.; Sun, Y.; Goswami, N.; Pal, S. K.; Balasubramanian, K.; Pradeep, T. Ag_7Au_6 : A 13-Atom Alloy Quantum Cluster. *Angew. Chem., Int. Ed.* **2012**, *51*, 2155–2159.
- (54) Henglein, A. Mechanism of Reactions on Colloidal Microelectrodes and Size Quantization Effects. In *Electrochemistry II*; Steckhan, E., Ed.; Springer: Berlin/Heidelberg, 1988; Vol. 143, pp 113–180.
- (55) Xu, Q.-Q.; Dong, X.-Y.; Huang, R.-W.; Li, B.; Zang, S.-Q.; Mak, T. C. W. A Thermochromic Silver Nanocluster Exhibiting Dual Emission Character. *Nanoscale* **2015**, *7*, 1650–1654.
- (56) Díez, I.; Pusa, M.; Kulmala, S.; Jiang, H.; Walther, A.; Goldmann, A. S.; Müller, A. H. E.; Ikkala, O.; Ras, R. H. A. Color Tunability and Electrochemiluminescence of Silver Nanoclusters. *Angew. Chem., Int. Ed.* **2009**, *48*, 2122–2125.
- (57) Bootharaju, M. S.; Burlakov, V. M.; Besong, T. M. D.; Joshi, C. P.; AbdulHalim, L. G.; Black, D.; Whetten, R.; Goriely, A.; Bakr, O. M. Reversible Size Control of Silver Nanoclusters via Ligand-exchange. *Chem. Mater.* **2015**, *27*, 4289–4297.
- (58) Cao, T.; Jin, S.; Wang, S.; Zhang, D.; Meng, X.; Zhu, M. A Comparison of the Chiral Counterion, Solvent, and Ligand Used to Induce a Chiroptical Response from Au_{25}^- Nanoclusters. *Nanoscale* **2013**, *5*, 7589–7595.
- (59) Farrag, M.; Tschurl, M.; Heiz, U. Chiral Gold and Silver Nanoclusters: Preparation, Size Selection, and Chiroptical Properties. *Chem. Mater.* **2013**, *25*, 862–870.
- (60) Chakraborty, I.; Pradeep, T. Reversible Formation of Ag_{44} From Selenolates. *Nanoscale* **2014**, *6*, 14190–14194.
- (61) Shichibu, Y.; Negishi, Y.; Watanabe, T.; Chaki, N. K.; Kawaguchi, H.; Tsukuda, T. Bicosahedral Gold Clusters $[\text{Au}_{25}(\text{PPh}_3)_{10}(\text{SC}_n\text{H}_{2n+1})_5\text{Cl}_2]^{2+}$ ($n=2–18$): A Stepping Stone to Cluster-Assembled Materials. *J. Phys. Chem. C* **2007**, *111*, 7845–7847.
- (62) Qian, H.; Zhu, M.; Lanni, E.; Zhu, Y.; Bier, M. E.; Jin, R. Conversion of Polydisperse Au Nanoparticles into Monodisperse Au_{25} Nanorods and Nanospheres. *J. Phys. Chem. C* **2009**, *113*, 17599–17603.
- (63) Zhu, Y.; Qian, H.; Das, A.; Jin, R. Comparison of the Catalytic Properties of 25-Atom Gold Nanospheres and Nanorods. *Chin. J. Catal.* **2011**, *32*, 1149–1155.
- (64) Yang, H.; Lei, J.; Wu, B.; Wang, Y.; Zhou, M.; Xia, A.; Zheng, L.; Zheng, N. Crystal Structure of a Luminescent Thiolated Ag Nanocluster with an Octahedral Ag_6^{4+} Core. *Chem. Commun.* **2013**, *49*, 300–302.
- (65) Yang, H.; Wang, Y.; Zheng, N. Stabilizing Subnanometer $\text{Ag}(0)$ Nanoclusters by Thiolate and Diphenylphosphine Ligands and Their Crystal Structures. *Nanoscale* **2013**, *5*, 2674–2677.
- (66) Tang, Q.; Ouyang, R.; Tian, Z.; Jiang, D.-e. The Ligand Effect on the Isomer Stability of $\text{Au}_{24}(\text{SR})_{20}$ Clusters. *Nanoscale* **2015**, *7*, 2225–2229.
- (67) Tlahuice-Flores, A.; Whetten, R. L.; Jose-Yacaman, M. Ligand Effects on the Structure and the Electronic Optical Properties of Anionic $\text{Au}_{25}(\text{SR})_{18}$ Clusters. *J. Phys. Chem. C* **2013**, *117*, 20867–20875.
- (68) Lopez-Acevedo, O.; Tsunoyama, H.; Tsukuda, T.; Häkkinen, H.; Aikens, C. M. Chirality and Electronic Structure of the Thiolate-Protected Au_{38} Nanocluster. *J. Am. Chem. Soc.* **2010**, *132*, 8210–8218.
- (69) Chakraborty, I.; Govindarajan, A.; Erusappan, J.; Ghosh, A.; Pradeep, T.; Yoon, B.; Whetten, R. L.; Landman, U. The Superstable 25 kDa Monolayer Protected Silver Nanoparticle: Measurements and Interpretation as an Icosahedral $\text{Ag}_{152}(\text{SCH}_2\text{CH}_2\text{Ph})_{60}$ Cluster. *Nano Lett.* **2012**, *12*, 5861–5866.
- (70) Kubo, R. Electronic Properties of Metallic Fine Particles. *I. J. Phys. Soc. Jpn.* **1962**, *17*, 975.
- (71) Buceta, D.; Piñeiro, Y.; Vázquez-Vázquez, C.; Rivas, J.; López-Quintela, M. Metallic Clusters: Theoretical Background, Properties and Synthesis in Microemulsions. *Catalysts* **2014**, *4*, 356–374.
- (72) Bigioni, T. P.; Whetten, R. L.; Dag, Ö. Near-Infrared Luminescence from Small Gold Nanocrystals. *J. Phys. Chem. B* **2000**, *104*, 6983–6986.
- (73) Wilcoxon, J. P.; Martin, J. E.; Parsapour, F.; Wiedenman, B.; Kelley, D. F. Photoluminescence from Nanosize Gold Clusters. *J. Chem. Phys.* **1998**, *108*, 9137–9143.
- (74) Link, S.; Beeby, A.; FitzGerald, S.; El-Sayed, M. A.; Schaaff, T. G.; Whetten, R. L. Visible to Infrared Luminescence from a 28-Atom Gold Cluster. *J. Phys. Chem. B* **2002**, *106*, 3410–3415.

- (75) Zheng, J.; Zhang, C.; Dickson, R. M. Highly Fluorescent, Water-Soluble, Size-Tunable Gold Quantum Dots. *Phys. Rev. Lett.* **2004**, *93*, 077402.
- (76) Zheng, J.; Dickson, R. M. Individual Water-Soluble Dendrimer-Encapsulated Silver Nanodot Fluorescence. *J. Am. Chem. Soc.* **2002**, *124*, 13982–13983.
- (77) Yuan, X.; Setyawati, M. I.; Tan, A. S.; Ong, C. N.; Leong, D. T.; Xie, J. Highly Luminescent Silver Nanoclusters with Tunable Emissions: Cyclic Reduction-Decomposition Synthesis and Antimicrobial Properties. *NPG Asia Mater.* **2013**, *5*, e39.
- (78) Li, B.; Huang, R.-W.; Qin, J.-H.; Zang, S.-Q.; Gao, G.-G.; Hou, H.-W.; Mak, T. C. W. Thermochromic Luminescent Nest-Like Silver Thiolate Cluster. *Chem. - Eur. J.* **2014**, *20*, 12416–12420.
- (79) Wu, Z.; Jin, R. On the Ligand's Role in the Fluorescence of Gold Nanoclusters. *Nano Lett.* **2010**, *10*, 2568–2573.
- (80) Pelton, M.; Tang, Y.; Bakr, O. M.; Stellacci, F. Long-Lived Charge-Separated States in Ligand-Stabilized Silver Clusters. *J. Am. Chem. Soc.* **2012**, *134*, 11856–11859.
- (81) Chin, P. T. K.; Linden, M. v. d.; Harten, E. J. v.; Barendregt, A.; Rood, M. T. M.; Koster, A. J.; Leeuwen, F. W. B. v.; Donega, C. d. M.; Heck, A. J. R.; Meijerink, A. Enhanced Luminescence of Ag Nanoclusters via Surface Modification. *Nanotechnology* **2013**, *24*, 075703.
- (82) Yao, Q.; Yu, Y.; Yuan, X.; Yu, Y.; Zhao, D.; Xie, J.; Lee, J. Y. Counterion-Assisted Shaping of Nanocluster Supracrystals. *Angew. Chem., Int. Ed.* **2015**, *54*, 184–189.
- (83) Das, A.; Li, T.; Nobusada, K.; Zeng, C.; Rosi, N. L.; Jin, R. Nonsuperatomic $[Au_{23}(SC_6H_{11})_{16}]^-$ Nanocluster Featuring Bipyramidal Au_{15} Kernel and Trimeric $Au_3(SR)_4$ Motif. *J. Am. Chem. Soc.* **2013**, *135*, 18264–18267.
- (84) Zeng, C.; Chen, Y.; Kirschbaum, K.; Appavoo, K.; Sfeir, M. Y.; Jin, R. Structural Patterns at All Scales in a Nonmetallic Chiral $Au_{133}(SR)_{52}$ Nanoparticle. *Science Advances* **2015**, *1*, e1500045.
- (85) Jena, P. Beyond the Periodic Table of Elements: The Role of Superatoms. *J. Phys. Chem. Lett.* **2013**, *4*, 1432–1442.
- (86) Luo, Z.; Castleman, A. W. Special and General Superatoms. *Acc. Chem. Res.* **2014**, *47*, 2931–2940.